Defect formation during deposition of undoped *a*-Si:H by rf glow discharge

Keiji Maeda, Ikurou Umezu,* and Hotaka Ishizuka
Department of Materials Science and Technology, Science University of Tokyo, Noda, Chiba 278, Japan
(Received 10 November 1995; revised 9 September 1996)

Dependence of the as-grown defect concentration in undoped *a*-Si:H deposited by rf glow discharge on the deposition parameters is investigated. It is found that the defect density behaves similarly to the concentration of SiH_2 configuration in the films deposited at substrate temperatures below 300 °C. The defect concentration varies proportionally to about the third to fourth power of the SiH_2 concentration depending on the deposition conditions. The Urbach energy increases in samples deposited under the condition where SiH_2 concentration increases. An additional energy is necessary to convert the weak bond in the valence-band tail into the defect. The observed characteristics are analyzed by a model in which this additional energy is produced by the surface reaction of SiH_3 incorporating the SiH_2 configuration into the network. These characteristics are compared with those of the Staebler-Wronski effect. The increase of weak bond density contributes to the increase of defect creation efficiency. The analyses give a quantitative explanation of the observed characteristics and estimation of some parameters involved in the conversion process. Similarities in the mechanisms are pointed out between the as-deposited defect formation and the Staebler-Wronski effect. [S0163-1829(97)10707-X]

I. INTRODUCTION

Hydrogenated amorphous silicon (*a*-Si:H) is usually deposited as a thin film by rf glow discharge of SiH_4 gas on a substrate kept at temperatures below 400 °C. Defects in undoped *a*-Si:H film are considered to be the Si dangling bonds (DB), although a controversy with the floating bond model has not been completely settled.[1] The concentration of Si DB in undoped *a*-Si:H film depends on the preparation conditions including heat treatment after deposition. Numerous investigations have been made to understand the correlation between the DB density N_s and the preparation conditions. In an early stage of research on plasma-deposited *a*-Si:H, it was revealed that there is a rapid increase of the defect density with an increase of hydrogen content as the coupled SiH_2 configuration.[2]

For the explanation of a decrease of N_s with decreasing equilibrium temperature by annealing, the idea that *a*-Si:H network is in a quasithermal equilibrium condition that is frozen during the cooling process has been successful.[3] A configuration involving the dangling bonds corresponds to a high-energy state. However, it has been observed experimentally that the as-deposited defect density increases with decreasing substrate temperature T_s during the deposition by two or three orders of magnitude with its minimum value at a temperature of about 250 °C.[4] It is considered that the defect density in the as-deposited state at low temperature is primarily determined by the deposition reaction.

A correlation has been found to exist between N_s and the Urbach energy E_U of the valence-band tail state.[5,6] When the Urbach energy becomes large, the density of states in the valence-band tail of comparable energy with the dangling bond increases. The thermal equilibrium relation between the weak bond and the defect seems to have been accepted.[5] However, as for the mechanisms of this correlation between N_s and E_U there remain several ambiguities. As discussed later, an additional energy seems necessary to create defects by breaking the weak bond. This energy is to be supplied from one of the surface reactions. This reaction has to possess some special characteristics: it must be dominant at low deposition temperatures and produce enough amount energy.

Recently, we proposed a mechanism of the surface reactions.[7] We investigated the H atom concentration in *a*-Si:H films deposited under various conditions. It was separated into the SiH concentration S_1 and the SiH_2 concentration S_2 by decomposition of the IR absorption spectra. Since the release of H atoms is an essential part of the surface reaction of incident SiH_3 radicals, the configurations of hydrogen atoms retained in the network are a clue to understanding how the reactions proceed. There are two kinds of surface reactions; one is incorporating SiH and the other is incorporating SiH_2 into the network. The latter becomes dominant at low deposition temperatures.

In this paper, we measured the defect density N_s in these films by electron spin resonance (ESR). We found similar behavior of $\log_{10}N_s$ and S_2 with changes in the deposition parameters; N_s varies exponentially with S_2. We also measured the Urbach energy E_U in these samples. E_U increases with the increase of S_2 and N_s at deposition temperatures below 250 °C. We discuss ambiguities involved in two previously proposed models[5,6] on the temperature dependence of as-grown defect at T_s below 250 °C. We propose a mechanism of the defect formation during deposition based on our surface reaction mechanism. First, the cause of correlation between N_s and S_2 is considered. According to our surface reaction mechanism, the bimolecular reaction of adsorbed radicals leading to the incorporation of the SiH_2 configuration is expected to accompany a reaction energy large enough to break a weak Si—Si bond. The observed characteristics of the DB formation during deposition are compared with those of the Staebler-Wronski (SW) effect.[8] The absolute value of the defect formation efficiency is in agreement with that of the SW effect. As for the exponential variation of N_s with S_2, analyses are made in terms of the Urbach

energy E_U leading to satisfactory results: the defect formation efficiency is proportional to the weak bond density. The configurational coordinate treatment is introduced in the analyses. Some parameters involved in the conversion process can be estimated.

The previously proposed mechanism of surface reaction is briefly described in Sec. II, since it forms the basis of this paper, but is quite different from the mechanisms so far reported.[9,10] Our experimental results on N_s and E_U are presented in Sec. III. Discussion on the previously proposed models[5,6] and proposal of our model on the as-grown N_s are made in Sec. IV. The observed characteristics are quantitatively analyzed by a comparison with those of the Staebler-Wronski effect and determination of some parameters involved in the defect formation process are made based on the mechanism in Sec. V. The conclusion is given in Sec. VI.

II. MECHANISM OF SURFACE REACTION

It is known that the precursor of SiH_4 plasma contributing to deposition is an SiH_3 radical in low rate depositions using low rf power density with a sufficient SiH_4 gas supply.[11] It is believed that an incident SiH_3 radical is first adsorbed and then migrates on the H atom terminated surface until it forms a Si-Si bond with the bulk.[12]

The *a*-Si:H films used in the experiments to investigate the surface reaction mechanism were prepared by PECVD of a SiH_4 and H_2 gas mixture in a capacitively coupled reactor. The gas pressure was 0.5 Torr in the reaction chamber and the rf power density was 0.07 W/cm^2. The conditions for the series of depositions varying either the substrate temperature T_s or the SiH_4 partial pressure P_s were as follows. For the variation of P_s, the total gas flow rate $[SiH_4]+[H_2]$ was kept constant at 100 sccm and T_s was 250 °C. P_s was varied from 0.25 to 0.50 Torr by varying the SiH_4 flow rate from 50 to 100 sccm. It was reported that the SiH_3 production frequency in a rf plasma of a H_2/SiH_4 gas mixture is independent of H_2 dilution.[13] Therefore, P_s of the gas mixture is proportional to the SiH_3 precursor density in the plasma. For the variation of T_s, the flow rate was fixed at 50 sccm for each SiH_4 and H_2 gas, and T_s was varied from 120° to 360 °C.

The deconvolution of the IR-absorption spectra for determining the H atom density was made using a personal computer under the assumptions that (1) the peaks in the spectral region from 2000 to 2090 cm^{-1} are due to the stretching mode of the Si—H configuration having a peak at around 2000 cm^{-1} and the Si═H_2 configuration having a peak at around 2090 cm^{-1}; and (2) the component spectrum has a Gaussian shape.[14] As for the proportional constant A converting the integrated absorption intensity to the atomic concentration, the values given by Langford *et al.*[15] were used; $A(SiH)=0.9\times10^{20}$ cm^{-2} and $A(SiH_2)=2.2\times10^{20}$ cm^{-2}.

Figure 1 shows the results. The concentrations of SiH and SiH_2 thus obtained are shown for the variation of P_s in Fig. 1(a), and for the variation of T_s in Fig. 1(b). The variation of S_1 and S_2 is in opposite directions under the variation of P_s and T_s. The variation of total H atom concentration with the deposition parameters is dominated by the variation of S_2 in samples prepared at $T_s<250$ °C and $P_s>0.3$ Torr.

There has been a large discrepancy in the concentration ratio of SiH to SiH_2 determined by IR and by nuclear magnetic resonance (NMR).[4] The concentration ratio by IR was obtained using an equal proportional constant A for SiH and SiH_2. The large H density with broad spectral component by NMR (Ref. 16) was attributed to the clustered SiH on internal surfaces of microvoid.[17] The concentration ratio obtained by IR using Langford's constant agrees quite well with that obtained by NMR. Therefore, an ambiguity involved in the previous analyses of H atom concentrations is remarkably decreased by reducing a large contribution of the indefinitely defined microvoid.

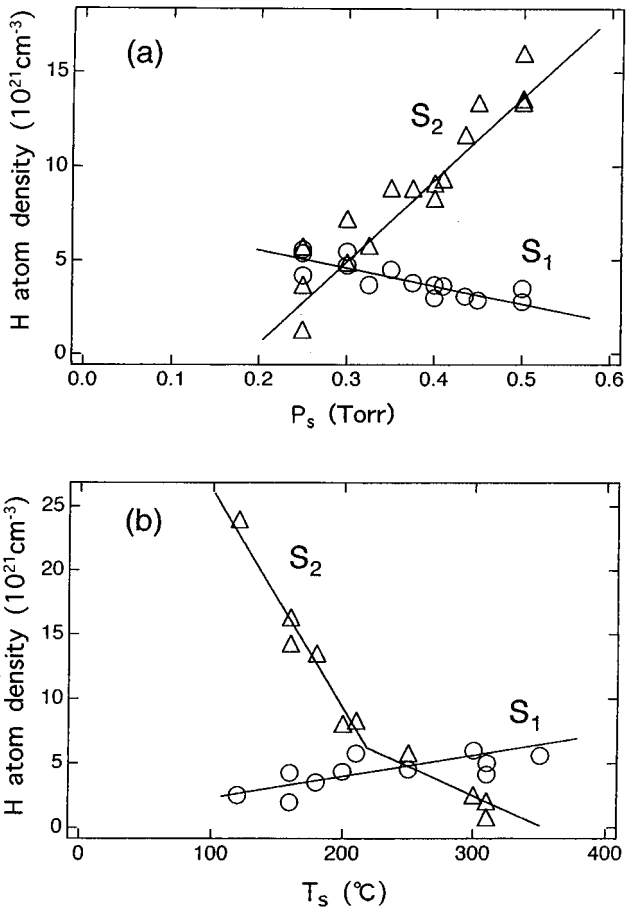

FIG. 1. H-atom densities in *a*-Si:H films. S_1 is SiH density (○) and S_2 is SiH_2 density (△). Films were (a) deposited by varying P_s, and (b) deposited by varying T_s.

The dependence of the deposition rate R on P_s and T_s was measured. R increases linearly with P_s when T_s is kept constant. This result coincides with the interpretation that only SiH_3 radicals derived from SiH_4 contribute to the growth of *a*-Si:H and that P_s is proportional to the precursor flux density incident upon the growing surface. The variation of S_2 as a function of P_s and T_s is plotted against the deposition rate R in Fig. 2. S_2 increases in both cases with increasing R, but quantitatively at a different rate depending on whether P_s or T_s is varied. This result, together with the result that S_1 and S_2 have opposite dependencies on P_s and T_s, can be understood if it is assumed that two different reaction processes are involved in the growth, and the variation of P_s and T_s has different effects on each reaction process.

For the analysis of the above experimental results, similar

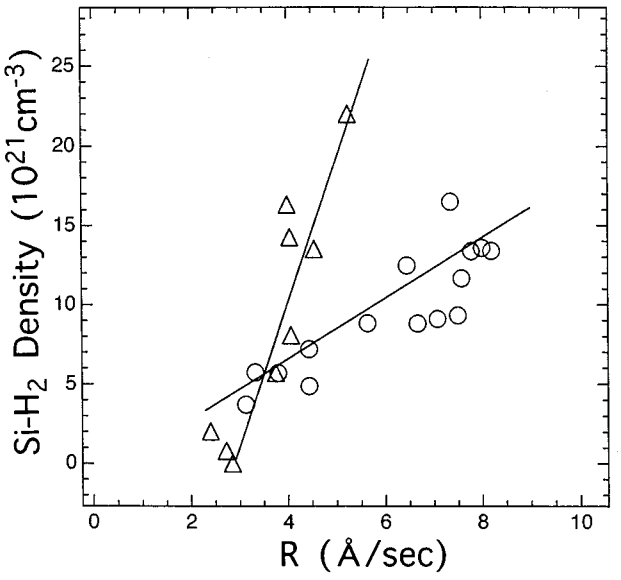

FIG. 2. SiH_2 density S_2 against deposition rate R. Films deposited varying P_s (○) and films deposited varying T_s (△).

phenomena treated by two well-known theories are recalled. One is the kinetics of crystal growth at different supersaturation, and the other is the kinetics of chemical reactions. While the lateral growth by single nucleation takes place in the crystal growth at low supersaturation, the vertical growth by multinucleation takes place at high supersaturation. According to the kinetic theory of chemical reactions, elementary reactions of different reaction order lead to different dependence of the reaction rate on the reaction parameters such as temperature and pressure.

We proposed the mechanism of surface reaction to explain the results of IR absorption.[7] These results cannot be explained by hitherto presented mechanisms.[9,10] There is a first-order, monomolecular process and a second-order, bimolecular process in the reaction of adsorbed SiH_3 radical. It is reasonable to associate the SiH_2 incorporation with the bimolecular reaction process of SiH_3 radicals, since S_2 is enhanced at high P_s, i.e., for high incident precursor flux density. The SiH incorporation is associated with the monomolecular process of SiH_3 radical, since S_1 becomes larger at higher T_s, where the diffusion of the adsorbed radical on the surface becomes active and it takes little time to arrive at a favorable site to form a Si—Si bond.

These two processes coexist and compete with each other under the conventional deposition conditions and a process with a short reaction time becomes the dominant process. While the bimolecular process becomes dominant at low T_s and under high P_s, the monomolecular process becomes dominant at high T_s and under low P_s. The deposition reaction by the bimolecular process incorporates an SiH_2 configuration for each Si atom in agreement with the H content in the film deposited at low temperatures.[2] The probability of incorporating an SiH configuration is small for a Si—Si bond formation by the monomolecular process at a steplike site on the growing surface.

By the analyses of the observed variation of S_2 with T_s and P_s based on this model, the activation energy of the surface diffusion of adsorbed SiH_3 radical on the growing surface is obtained to be 0.3 eV. This value is close to the previously estimated value of 0.2 eV.[18] The jumping frequency in the diffusion is a reasonable value. The data of S_1 variation are also analyzed and the minimum concentration of H atoms is found to be about 10 at. % in agreement with experiment.[7]

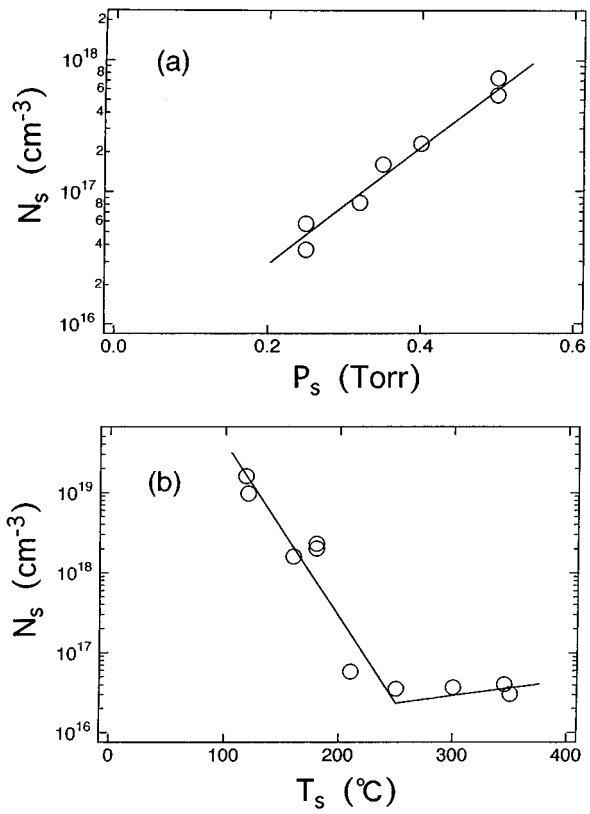

FIG. 3. Variation of defect density N_s with deposition conditions. (a) Films deposited varying P_s and (b) films deposited varying T_s.

III. EXPERIMENTAL RESULTS

The defect concentration N_s was measured by ESR using an X-band apparatus in the dark at room temperature. The dangling bond has an ESR absorption band at $g=2.0055$. The same kinds of samples were used as in the IR absorption. For several samples with small ESR signal intensity, the thickness dependence of the ESR signal intensity was measured to obtain the bulk defect density excluding possible surface contributions. The variation of N_s with P_s and T_s is shown in Fig. 3. N_s decreases rapidly with increasing temperature up to 250 °C, where it has a minimum value. Then, N_s increases slowly with increasing temperature. The temperature dependence of N_s is in agreement with reported results.[2,4] N_s increases with increasing P_s. $\log_{10}N_s$ behaves similarly to S_2 shown in Fig. 1 in the samples deposited at $T_s<250$ °C. While the temperature dependence at $T_s>300$ °C can be explained by an assumption of thermal equilibrium at the deposition temperature, the temperature dependence at $T_s<250$ °C cannot be explained by the same assumption.

While the variations of N_s and S_2 with the deposition

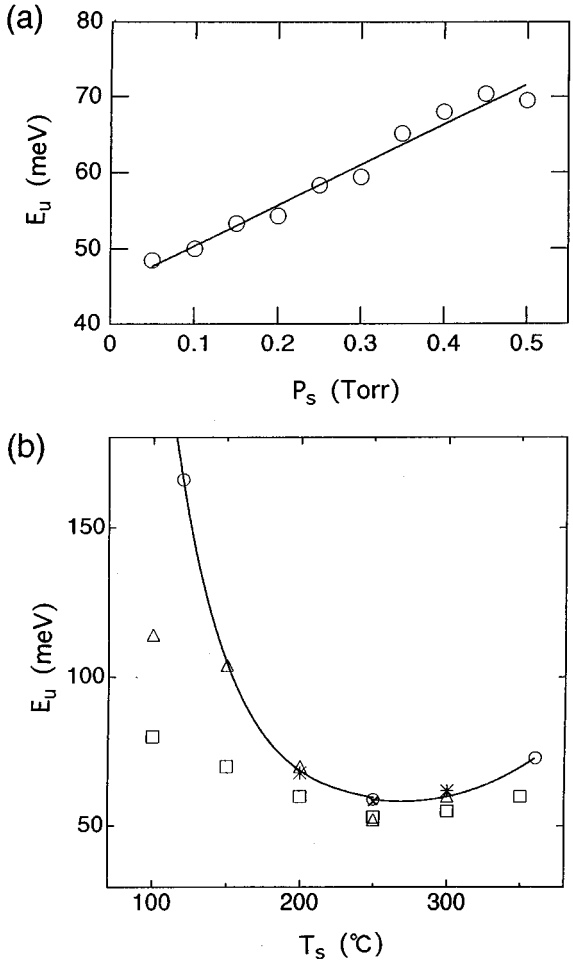

FIG. 4. Variation of Urbach energy E_U with deposition conditions. (a) Films deposited varying P_s and (b) films deposited varying T_s. In addition to our data (○), published data are also shown in (b): Kida *et al.* (Ref. 21, △), Nonomura *et al.* (Ref. 22, ∗), Roxlo (Ref. 23, ×), and Yamasaki (Ref. 24, □).

parameters are qualitatively similar, the greatest difference is that N_s is plotted on a logarithmic scale in Fig. 3 and S_2 is plotted on a linear scale in Fig. 1. It has been reported that the Urbach energy E_U of the valence-band tail state is correlated with N_s in the films deposited at T_s below 250 °C.[5,6] It is plausible that a variation of E_U is associated with an exponential variation of N_s. We measured E_U in our samples by the photothermal deflection spectroscopy (PDS) method.[19]

In Fig. 4, E_U is plotted against the variations of P_s and T_s in the preparation condition. The E_U value in the samples deposited at $T_s=250$ °C varies linearly with P_s and extrapolates to 45 meV at $P_s=0$ in agreement with the variation of E_U with the deposition rate by rf power density.[20] For the variation with T_s, reported values of E_U are also plotted.[21–24] The variation of E_U with T_s below 250 °C is large compared with that above 250 °C. While the present results in the sample deposited at $T_s>250$ °C agree with the reported values, the results in the samples deposited at $T_s<250$ °C do not agree. This seems to indicate that E_U is determined in thermal equilibrium at $T_s>250$ °C but E_U depends on the preparation conditions at $T_s<250$ °C. Yamasaki[24] measured E_U by the photoacoustic spectroscopy (PAS) technique. He prepared his samples shown in Fig. 4 under low SiH_4 pressure of 50 mTorr at low rf power density of 30 mW cm^{-2}. The H atom content in his sample prepared at $T_s=100$ °C is only 24 at. %. Kida *et al.*[21] reported rather small E_U values shown in Fig. 4. They obtained their results by the primary photocurrent technique. It is considered that their data may underestimate the value of E_U.[5]

It is considered that E_U reflects disorder broadening in a-Si:H. The increase of E_U in our samples is larger in the T_s variation than in the P_s variation for nearly equal increases of S_2 in the two variations. However, it was reported that the increase of E_U with decreasing T_s is rather small in the sample of low N_s and hydrogen contents[24] as shown in Fig. 4. These results seem to imply that S_2 is one of the major factors determining the disorder in the samples deposited at temperatures below the freezing temperature.

IV. MECHANISM OF DEFECT FORMATION

Two models have been proposed to explain the increase of N_s with increasing E_U at T_s below 250 °C.[5,6] A state containing a DB has an energy U_B higher than the state without DB. When a weak bond in the tail state of high energy is considered as the initial state of bond breaking, U_B becomes small. The state density distribution $N_T(E)$ in the valence-band tail is given by

$$N_T(E)=N_v^{\mu}\exp[-(E-E_v)/E_U], \tag{1}$$

where N_v^{μ} is the tail state density at the mobility edge of the valence band of energy E_v. Therefore, there are many initial states with small U_B for the bond breaking in samples of large E_U.

Smith and Wagner[5] proposed a model for the deposition at $T_s<250$ °C in which the tail states of equal energy to the dangling bond are guaranteed to convert to the dangling bond. They set N_s equal to the tail-state density given by integrating Eq. (1),

$$N_{\mathrm{TD}}=\int_{E_D}^{\infty}N_T(E)dE=N_v^{\mu}E_U\exp[-(E_D-E_v)/E_U]. \tag{2}$$

Since the observed E_U increases with decreasing T_s, N_s increases exponentially with decreasing T_s. However, such a conversion is only possible in thermal equilibrium, if there is a potential-energy barrier between the tail state and the DB state as is usually the case. The freezing temperature T_F of undoped a-Si:H is known to be about 200 °C.[3,25] At temperatures below T_F it is difficult to reach thermal equilibrium.[6] The increase of E_U at low temperatures implies that an increasing number of constituent atoms are becoming trapped in the small and disordered potential. In such a situation it is not guaranteed to consider the thermal equilibrium between the weak bond and the defect.

Stutzmann[6] ignored the potential-energy barrier and proposed a model in which the bonding states of the valence-band tail break spontaneously when the tail states are in an energy level equal to the energy E_D of DB. The value of E_D-E_v in Eq. (2) is important for the propriety of the model. It was determined to be 0.55 eV by fitting Eq. (2) with experimental data.[6] This value seems to be much

smaller than the generally accepted value.[1] The band gap between the conduction band and the valence band is approximately 1.85 eV in undoped *a*-Si:H. The gap state energy of the native defect in *n*-type *a*-Si:H is 0.8–0.9 eV below E_c. While the correlation energy in the DB is not known accurately, it is considered to be positive and 0.1–0.2 eV. Therefore, $E_D - E_v$ is estimated to be about 0.8 eV.

Furthermore, a following ambiguity arises for this model, which assumes the existence of the tail state of density $N_T(E)$expressed by Eq. (1) up to $E > E_D$. If we consider the dehydrogenation of a SiH_3 precursor radical in the network formation process, such a sequence of unstable Si—Si bond formation and spontaneous breaking, i.e., a reaction of two Si—H bonds leading to spontaneous production of a H_2 molecule and two dangling bonds, is very unlikely to take place on account of the reaction energy estimated from the bond energies given below; enthalpy increase by this reaction is estimated to be 33.6 kcal/mol=1.6 eV. It seems likely that the tail state that breaks spontaneously does not extend to energies higher than E_D.

It is inferred from the above discussions that an additional energy supply is needed to break a Si—Si bond in the tail state. This additional energy can be produced by the heat of reaction, i.e., the enthalpy change in the deposition reaction. In order for the reaction to proceed spontaneously, a change in the Gibbs free energy should be negative for the reaction. Since a contribution of the entropy term is not considered to be important in the deposition reaction, the Gibbs free energy change can be approximated by the enthalpy change. In Ref. 7, the enthalpy change or heat of reaction was calculated for the monomolecular and the bimolecular reactions. It was noted that the enthalpy change accompanying the bimolecular reaction is much larger than the monomolecular reaction.

The following bond energies were given by Pauling:[26] Si—H bond 70.4 kcal/mol, Si—Si bond 42.2 kcal/mol, and H—H bond 104.2 kcal/mol. The adsorption energy of a SiH_3 radical on an H atom terminating the growing surface, Si·H—Si, was assumed to be 10 kcal/mol, which is reasonable in comparison with the activation energy 0.3 eV of the surface diffusion coefficient.[7] As an example of the monomolecular reaction of an adsorbed radical, the reaction at a steplike site shown in Fig. 5(a) is considered in an analogy with the crystal growth. The steplike site in amorphous material does not mean a site linearly aligned on the growing surface. The Si atom in a diffusing radical assumes a stable position of low potential energy by forming two Si—Si bonds simultaneously with the network at this site. In this reaction, three Si—H bonds, and an adsorption of Si on H, Si·H—Si, disappear and two Si—Si bonds and 3/2 H—H bonds are formed. The enthalpy change $-\Delta H_M$ by this monomolecular reaction is calculated to be 20 kcal=0.87 eV.

For the bimolecular reaction, clustering of two SiH_3 radicals on a flat surface is considered in analogy with the crystal growth. Each Si atom in SiH_3 radicals becomes stabilized by simultaneously forming two Si—Si bonds to the network. It is difficult to illustrate the reaction precisely, but one of the reactions incorporating the SiH_2 configuration is presumably represented by Fig. 5(b). By this reaction, four Si—H bonds and two adsorptions of Si on H disappear. Three Si—Si bonds are formed and two H_2 molecules are released. The enthalpy change in this bimolecular reaction is $-\Delta H_B = 34$ kcal=1.48 eV.

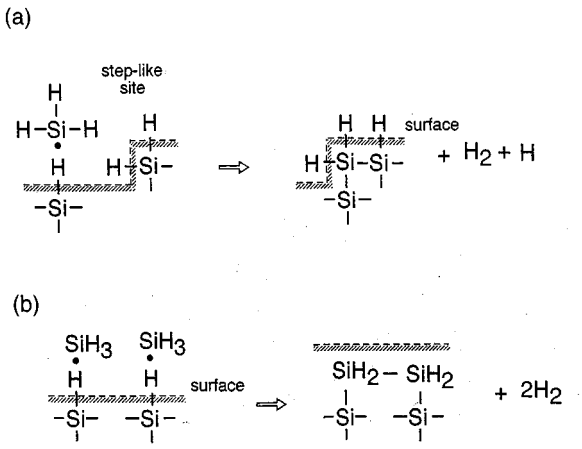

FIG. 5. Examples of surface reaction of adsorbed SiH_3 radical. (a) Monomolecular reaction at steplike site, and (b) bimolecular reaction on flat surface. Growing surface is indicated.

Although the exact enthalpy change depends on the reaction involved, the enthalpy change in the bimolecular reaction $-\Delta H_B$ is larger than that in the monomolecular reaction $-\Delta H_M$. The reason is that the number of bonds, which are broken and formed in the reaction, is larger in the bimolecular reaction than in the monomolecular reaction and that the average enthalpy change by bond rearrangement, i.e., by breaking two Si—H bonds and forming a Si—Si bond and a H—H bond, is negative, −6 kcal.

V. COMPARISON WITH STAEBLER-WRONSKI EFFECT

A. Defect creation efficiency

For a discussion on the mechanism of the Si—Si bond breaking, comparison with a similar phenomenon is indispensable. While there has been some debate about the interpretation of the Staebler-Wronski (SW) effect, the bond breaking model is considered to be the most reliable one at this time.[1,27] According to the Si—Si bond breaking model, this effect is understood as follows.[8] Figure 6(a) shows the energy band diagram of undoped *a*-Si:H. As described in the preceding section, the energy level of the Si DB in undoped *a*-Si:H is about 0.8 eV above the valence-band mobility edge E_v in the band gap E_g of 1.85 eV. The valence-band tail is broadened by the Urbach energy due to the irregularity of the amorphous network.

When an electron-hole pair produced by light illumination radiatively recombines, the excess energy U is emitted as a luminescent photon. Weak Si—Si bonds in the Urbach tail are broken if the excess energy is enough to raise electrons in the valence-band tail over the potential-energy barrier to the dangling bond level as illustrated in Fig. 6(b). Since a weak Si—Si bond is comprised of two electrons, the energy difference between the two minima in the potential energy is twice the energy difference ΔE_s between the DB energy E_D and the Urbach tail energy E_o. An extra energy α is expected to be necessary to surmount the potential-energy barrier separating the two minimum positions in the configu-

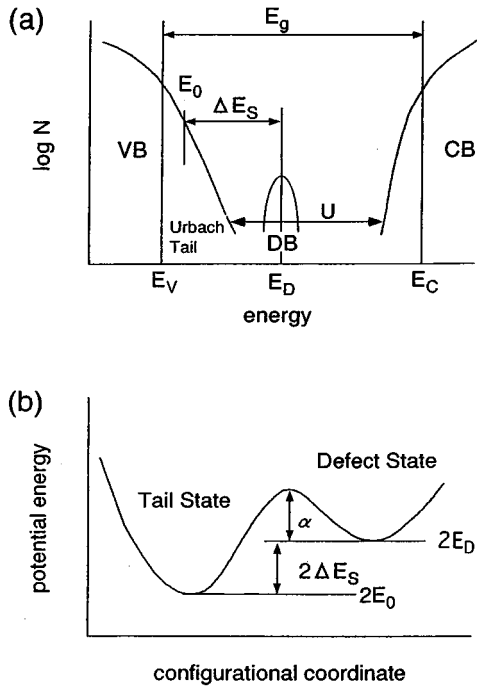

FIG. 6. (a) Energy band diagram of undoped a-Si:H. U is the energy emitted by tail-to-tail recombination, ΔE_s is the energy difference between dangling bond DB and Urbach tail E_o and N is the state density. (b) Configurational coordinate diagram of tail state and defect state separated by a potential-energy barrier.

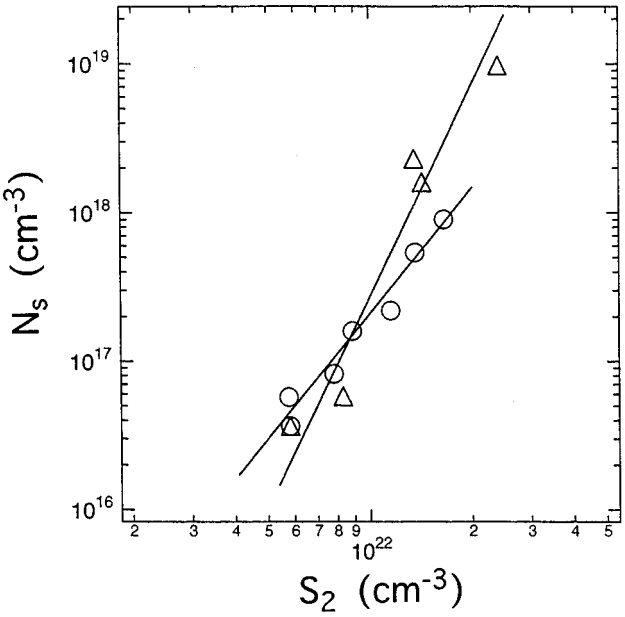

FIG. 7. Dependence of defect density N_s on SiH_2 density S_2. Films deposited varying P_s (○) and films deposited varying T_s (△).

rational coordinate diagram. Thus, the excess energy U_b necessary to break a weak bond becomes $U_b = 2\Delta E_s + \alpha$.

The energy for breaking a weak bond of $2\Delta E_s + \alpha$ is usually considered to be 1.3–1.4 eV from the tail-to-tail luminescence energy U.[28] This energy is a little smaller than the enthalpy change by the bimolecular reaction $-\Delta H_B$ but is larger than the enthalpy change by the monomolecular reaction $-\Delta H_M$; i.e.,

$$-\Delta H_B > U > -\Delta H_M . \tag{3}$$

Therefore, it can be considered that the breaking of a weak bond occurs by the energy of a bimolecular reaction but not by the energy of a monomolecular reaction. This is in agreement with the experimental result that N_s increases with increasing S_2, which is incorporated by the bimolecular reaction for either variation of P_s or T_s in the deposition parameters.

Since the Frank-Condon principle applies in this case, i.e., the optical energy difference in light emission process is smaller than the energy difference in equilibrium, the supplied energy in the SW effect is expected to be larger than U. Then U_b is set equal to $-\Delta H_B$. The relation among several energies discussed above becomes

$$-\Delta H_B = 2(E_D - E_o) + \alpha. \tag{4}$$

While there are many uncertainties, Eq. (4) becomes under the assumption $-\Delta H_B = 1.5$ eV and $E_D - D_v = 0.8$ eV

$$E_o - E_v = (\alpha + 0.1\ \text{eV})/2. \tag{5}$$

The exponential dependence of tail state density on energy is observed over the range of $(E - E_v) = 0.2$–0.5 eV.[29] The above relation is reasonable with regard to the value of α in the situation where the tail state density is closely correlated with the defect creation efficiency.

The defect creation efficiency in the SW effect by the energy of tail-to-tail recombination of an electron-hole pair was defined by Stutzmann, Jackson, and Tsai as the energy transfer efficiency.[8] They described the rate of DB creation with the illumination time t_{ill} by

$$dN_s/dt_{\text{ill}} = c_{\text{SW}} A_t np. \tag{6}$$

Here, $A_t np$ is the number of tail-to-tail recombination per unit time and volume, and c_{SW} is a constant describing the average efficiency of these transitions for the creation of new DB. They evaluated c_{SW} experimentally to be 5×10^{-5}.

The N_s versus S_2 relation in our study is shown in Fig. 7 for the two series of samples, one deposited at various T_s and the other deposited under various P_s. The variation of N_s with T_s is larger than that with P_s. From the gradient of the experimental points, N_s is proportional to the 4.4th power of S_2 when T_s is varied and is proportional to the 2.9th power of S_2 when P_s is varied. This results also indicates that the defect creation efficiency by energy transfer is correlated with the density of weak bond since the variation of Urbach energy was observed. The ratio N_s/S_2 in our experiment is in a range of 5×10^{-4} to 6×10^{-6} as can be obtained from Fig. 7. A defect is considered to be created by a bimolecular reaction process incorporating four S_2 hydrogen atoms. Then, c_{SW} in the present evaluation is equal to $4N_s/S_2 = 2.0\times10^{-3}$ to 2.4×10^{-5}. The value of c_{SW} is associated with the tail state density expressed by Eq. (1). It becomes larger for larger E_U and smaller $E_o - E_v$. Hence, c_{SW} becomes larger in our study using samples of larger E_U. From the above discussion it becomes clear that the absolute mag-

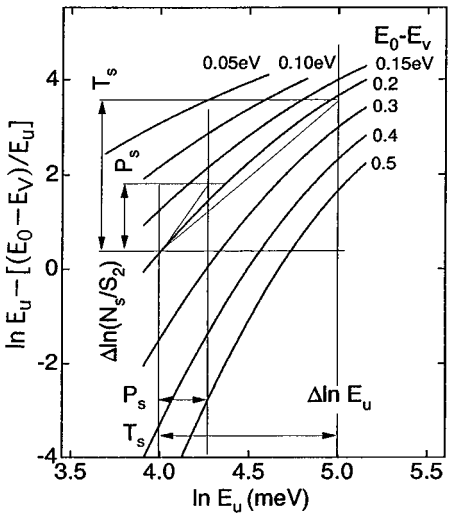

FIG. 8. $\ln E_U - [(E_o - E_v)/E_U]$ plotted against $\ln E_U$ for various $E_o - E_v$ values. The ranges of $\ln E_U$ with variations of T_s and P_s are indicated horizontally. The ranges of variation of $\ln(N_s/S_2)$ with variations of T_s and P_s are indicated vertically. The gradient of hypotenuse in the triangles with $\Delta \ln E_U$ and $\Delta \ln(N_s/S_2)$ is compared with the calculated curves.

nitude of the defect creation efficiency is in agreement with the SW effect. The dependence of N_s on S_2 is discussed in the following.

The energy transfer process from chemical reaction to a weak bond has to be considered. An excited bonding state is conceivable to be produced due to the excess energy at the reaction site. This excited state can migrate some distance in the network as an electron-hole pair, but is unable to move around through the network since the energy is less than the band gap energy. The depth of the defect formation is considered to be only a few atomic layers thick. The weak bond satisfying the condition given by Eq. (5) within this region can be converted to the defect by the energy supply.

The variation of N_s with higher power of S_2 than the linear is considered to be due to the variation of this weak bond density with deposition conditions. The ratio N_s/S_2 is expected to be proportional to the weak bond density obtained by integrating Eq. (1) between E_o and infinity similarly to Eq. (2). In order to estimate the variation of the weak bond density, the value of $(E_o - E_v)$ is needed. We plotted the calculated values of $\ln E_U - [(E_o - E_v)/E_U]$ against $\ln E_U$ in Fig. 8 for various values of $(E_o - E_v)$ as a parameter. The observed ranges of Urbach energy, $\Delta \ln E_U$, are indicated horizontally in this figure for the variation of T_s (120–250 °C) and P_s (0.25–0.50 Torr) for increasing E_U from its minimum value shown in Fig. 4. The logarithmic ranges of observed variation $\Delta \ln(N_s/S_2)$ are also indicated vertically in this figure for the variations of T_s and P_s. The hypotenuse making a rectangular triangle with $\Delta \ln(N_s/S_2)$and $\Delta \ln E_U$ can be drawn in the figure for the variation of T_s and P_s, respectively. Since the variation of $\ln(N_s/S_2)$ has a meaning for this purpose, the triangles can be shifted vertically in this figure.

The $(E_o - E_v)$ value can be determined of which curve has the same gradient to the hypotenuse of the T_s and P_s triangle, respectively. The curve of $E_o - E_v = 0.2$ eV gives the best fit for both T_s and P_s variations as shown in Fig. 8. This value is small compared with $E_D - E_v$ values in the previous models; 0.85 eV by Smith and Wagner[5] and 0.55 eV by Stutzmann.[6] The difference has the numerical effect of compensating the smallness of the defect creation efficiency introduced into the present model. The potential barrier height α in the configurational coordinate diagram shown in Fig. 6(b) is then estimated to be approximately 0.3 eV by Eq. (5). Therefore, the characteristics of as-deposited defect density can be quantitatively represented by

$$N_s = C_s S_2 E_U \exp[-(E_o - E_v)/E_U], \tag{7}$$

where C_s is a proportional constant, which involves the defect creation efficiency by energy transfer.

B. Similarity and difference in characteristics

The dependence of DB density N_{SW} introduced by the SW effect on the hydrogen atom density indicates the similarity in the mechanism between the defect formation during deposition at low T_s and the SW effect. It was reported[30] that the light-induced degradation of photoconductivity decreases when the SiH_2 bond density decreases in a-Si films deposited at $T_s = 200$ °C with a low impurity content of around 10^{18} cm^{-3}. There is no strong relationship between the light-induced degradation and the SiH bond density.

Bhattacharya and Mahan[31] reported that the logarithm of the PDS signal intensity due to defects induced by the SW effect is correlated with the 2070-cm^{-1} IR absorption of the film. They defined the microstructure fraction F_m by

$$F_m = [2070]/\{[2000] + [2070]\},$$

where the brackets denote the integrated band intensities of the respective IR absorption. Since the proportional constant converting the absorption intensity to the atomic concentration is different for the 2000- and the 2070-cm^{-1} absorption bands,[15] their definition of the microstructure fraction related with the density deficiency by F_m becomes ambiguous. According to their data, E_U varies proportionally to F_m. Their data of the N_{SW} versus E_U relation are plotted in Fig. 9. The light soaking was made for 22 h under an ELH lamp calibrated to 100 mW/cm^2 on a-Si:H films of 1–2 μm thick deposited at $T_s \geqslant 250$ °C. There is a correlation that $\log_{10} N_{SW}$ varies proportionally to E_U.Therefore, their data seem to indicate that the bond breaking by the SW effect occurs preferentially at the weak bond induced by the introduction of SiH_2 configuration into the network.

Since N_{SW} under the same light soaking in the SW effect is proportional to N_s/S_2 of as-deposited defects, the $\ln(N_s/S_2)$ versus $\ln E_U$ plot in Fig. 8 is expected to be also applicable in this case. A plot of the variation of $\ln N_{SW}$ with E_U shown by the straight line in Fig. 9 is made in the same way as in Fig. 8. The curve of $E_o - E_v = 0.10$ eV gives the best fit to the data. The weaker dependence of N_{SW} on E_U in the SW effect compared with the as-deposited defects leads to the smaller value of $E_o - E_U$.

The most important difference between the as-grown defects and the Staebler-Wronski defects is the thermal stability. The defects due to the SW effect are usually produced at room temperature and disappear by thermal annealing at temperatures between 150 and 200 °C.[8] On the other hand,

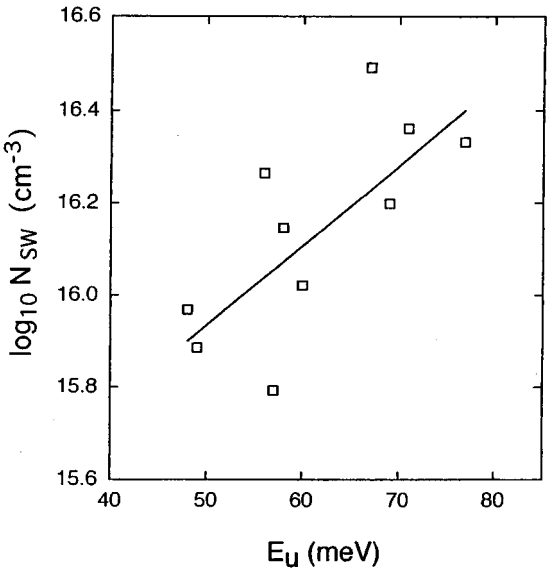

FIG. 9. Logarithm of defect density N_{SW} produced by the SW effect vs Urbach energy E_U for different a-Si:H samples. (See Bhattacharya and Mahan, Ref. 31).

the defect density in the as-deposited state decreases very slowly by annealing at temperatures below 250 °C.[32] An appreciable annealing occurs at temperatures of about 300 °C and above.

A cause of this difference is considered as follows. The defect produced by the Staebler-Wronski effect is subject to constriction in the bulk due to a deviation from the initial network. Although some local atomic relaxations are made avoiding instantaneous restoration, the restoring force to the initial low-energy state is still operating. Therefore, the DB produced by the Staebler-Wronski effect disappears by an annealing at relatively low temperatures. On the other hand, the restoring force is weak for the defect introduced during deposition at a few atomic layers of depth under the growing surface at deposition temperature. The surrounding network has not yet become completely rigid for the DB. The restoring force to the initial state is largely relaxed during the succeeding deposition process on the strained surface.

By the above comparison with the Staebler-Wronski effect it becomes most likely that the as-grown defects are formed during deposition at temperatures below 300 °C owing to the enthalpy change accompanying the bimolecular reaction. The present simplified model is developed on the basis of our assumptions that the H atom concentration on the surface of a microvoid can be neglected and that the surface reaction is described by the two kinds of processes. However, a very large S_2 in films deposited at very low T_s might produce the microvoid. The IR absorption spectra of the Si—H bond terminating the growing surface[33] revealed that the dominant bonding configuration changes with decreasing temperature from SiH at 315 °C to SiH_2 and to SiH_3 at 25 °C. Such a change of H atom configuration in the surface termination might be related with a change of the surface reaction at very low T_s.

The mechanisms of the Staebler-Wronski effect and the as-deposited defect formation at low temperatures are very similar. The reason they have not been compared closely is considered as follows. In the studies of the Staebler-Wronski effect, the energy source, i.e., light illumination, has been emphasized. On the other hand, in the studies of as-deposited defect density at low temperatures, the material condition, i.e., the Urbach energy, has been emphasized; but both necessity and the presence of the energy source to break the weak bond have been disregarded.

VI. CONCLUSION

The dependence of the as-deposited defect density in undoped a-Si:H deposited at substrate temperatures below 300 °C by rf discharge is found experimentally to be similar to that of SiH_2 concentration. An additional energy supply seems necessary to create defect by breaking the weak bond. Based on the surface reaction mechanism proposed previously the characteristics of defect formation during deposition are compared with those of the Staebler-Wronski effect. Since the analyses give a quantitative explanation of the observed characteristics, it is concluded that the as-deposited defects are most likely formed near the growing surface during deposition owing to the enthalpy change accompanying the bimolecular reaction of adsorbed SiH_3 radicals incorporating a SiH_2 configuration into the network. The exponential increase of defect density with the increase of SiH_2 concentration is due to the associated increase of the weak bond density in the valence-band tail, which is converted to the defect. Finally, similarities in the mechanisms are pointed out between the as-deposited defect formation and the Staebler-Wronski effect.

ACKNOWLEDGMENTS

The authors thank H. Horigome for his PDS measurements and Dr. H. Okushi for his critical reading of the manuscript.

*Present address: Department of Applied Physics, Konan University, Okamoto, Higashinada-ku, Kobe 658, Japan.

[1] R. A. Street, *Hydrogenated Amorphous Silicon* (Cambridge University Press, Cambridge, 1991).
[2] J. C. Knights, G. Lucovsky, and R. J. Nemanich, J. Non-Cryst. Solids **32**, 393 (1979).
[3] R. A. Street and K. Winer, Phys. Rev. B **40**, 6236 (1989).
[4] T. Shimizu, K. Nakazawa, M. Kumeda, and S. Ueda, Physica B and C **117B&118B**, 926 (1983).
[5] Z. E. Smith and S. Wagner, Phys. Rev. Lett. **59**, 688 (1987).
[6] M. Stutzmann, Philos. Mag. B **60**, 531 (1989).
[7] K. Maeda, A. Kuroe, and A. Umezu, Phys. Rev. B **51**, 10 635 (1995).
[8] M. Stutzmann, W. B. Jackson, and C. C. Tsai, Phys. Rev. B **32**, 23 (1985).
[9] G. H. Lin, J. R. Doyle, M. He, and A. Gallagher, J. Appl. Phys. **64**, 188 (1988).
[10] G. Ganguly and A. Matsuda, Phys. Rev. B **47**, 3661 (1993); J. Non-Cryst. Solids **164-166**, 31 (1993).
[11] N. Itabashi, N. Nishiwaki, M. Magane, S. Naito, T. Goto, A. Matsuda, C. Yamada, and E. Hirota, Jpn. J. Appl. Phys. **29**, L505 (1990).

[12] A. Matsuda, K. Nomoto, Y. Takeuchi, A. Suzuki, A. Yuuki, and J. Perrin, Surf. Sci. **227**, 50 (1990).
[13] H. Nomura, A. Kono, and T. Goto, Jpn. J. Appl. Phys. **33**, 4165 (1994).
[14] In the description of the spectral width in Ref. 7, FWHM should read HWHM (half width at half maximum) on p. 10 638 both in the text and in Fig. 3.
[15] A. A. Langford, M. L. Fleet, B. B. Nelson, W. A. Langford, and N. Maley, Phys. Rev. B **45**, 13 367 (1992).
[16] J. A. Reimer, J. Phys. (Paris) Colloq. **42**, C4-715 (1981).
[17] J. Baum, K. K. Gleason, A. Pines, A. N. Garroway, and J. A. Reimer, Phys Rev. Lett. **56**, 1377 (1986).
[18] J.-L. Guizot, K. Nomoto, and A. Matsuda, Surf. Sci. **244**, 22 (1991).
[19] I. Umezu, M. Daigo, and K. Maeda, Jpn. J. Appl. Phys. **33**, L873 (1994).
[20] W. B. Jackson and N. M. Amer, Phys. Rev. B **25**, 5559 (1982).
[21] H. Kida, H. Yamagishi, T. Kamada, H. Okamoto, and Y. Hamakawa, in *First International Photovoltaic Science and Engineering Conference*, edited by M. Konagai (Nippon, Tokyo, 1984), p. 417.
[22] S. Nonomura, S. Sakata, T. Kamada, H. Kida, D. Kruangam, H. Okamoto, and Y. Hamakawa, J. Non-Cryst. Solids **77&78**, 865 (1985).
[23] C. Roxlo, as quoted by G. D. Cody, in *Semiconductors and Semimetals*, edited by J. Pankove (Academic, Orlando, 1984), Vol. 21-B, p. 11.
[24] S. Yamasaki, Philos. Mag. B **56**, 79 (1987).
[25] T. J. McMahon and R. Tsu, Appl. Phys. Lett. **51**, 412 (1987).
[26] L. Pauling, *The Nature of the Chemical Bond*, 3rd ed. (Cornell University Press, Ithaca, NY, 1960).
[27] T. Shimizu, J. Non-Cryst. Solids **164-166**, 163 (1993).
[28] R. A. Street, J. C. Knights, and D. K. Biegelsen, Phys. Rev. B **18**, 1880 (1978).
[29] K. Winer, I. Hirabayashi, and L. Ley, Phys. Rev. B **38**, 7680 (1988).
[30] N. Nakamura, T. Takahama, M. Isomura, M. Nishikuni, K. Yoshida, S. Tsuda, S. Nakano, M. Ohnishi, and Y. Kuwano, Jpn. J. Appl. Phys. **28**, 1762 (1989).
[31] E. Bhattacharya and A. H. Mahan, Appl. Phys. Lett. **52**, 1587 (1988).
[32] K. Tanaka and A. Matsuda, Mater. Sci. Rep. **2**, 139 (1987).
[33] Y. Toyoshima, K. Arai, A. Matsuda, and K. Tanaka, J. Non-Cryst. Solids **137-138**, 756 (1991).